Journal of Analytical and Applied Pyrolysis 105 (2014) 43–48

Contents lists available at ScienceDirect

Journal of Analytical and Applied Pyrolysis

journal homepage: www.elsevier.com/locate/jaap

Thermal analysis and products distribution of dried sewage sludge pyrolysis

Ningbo Gao[a,b], Juanjuan Li[a], Benyu Qi[a], Aimin Li[a,*], Yue Duan[b], Ze Wang[b]

[a] School of Environmental Science & Technology, Dalian University of Technology, Key Laboratory of Industrial Ecology and Environmental Engineering, MOE, Dalian 116024, China
[b] Institute of Process Engineering, Chinese Academy of Sciences, State Key Laboratory of Multiphase Complex Systems, Beijing 100190, China

ARTICLE INFO

Article history:
Received 22 July 2013
Accepted 5 October 2013
Available online 16 October 2013

Keywords:
Sewage sludge
Pyrolysis
XRF
TG–FTIR

ABSTRACT

Pyrolysis behavior of dried sewage sludge was studied by thermogravimetric–Fourier transforms infrared analysis (TG–FTIR) and differential scanning calorimetry (DSC) to investigate thermal decomposition and kinetics analysis. A tubular pyrolyzer was used to explore the production distribution of dried sewage sludge pyrolysis under different runs. The results showed that two weight loss peaks were presented in pyrolysis reaction in the ranges of 186–296 °C and 296–518 °C, and the activation energy of each stage was 82.284 kJ mol^{-1} and 48.342 kJ mol^{-1}, respectively. The main gases identified by FTIR analysis were CH_4, CO_2, CO and organic volatile compounds such as aldehydes, acids, alcohols and phenols. Under fast pyrolysis of dried sewage sludge, the maximum tar yield obtained was 46.14% at the temperature of 550 °C. The concentrations of all gases increased steadily with increasing pyrolysis temperature from 450 °C to 650 °C except for CO_2.

1. Introduction

Sewage sludge is the major byproduct in the wastewater treatment plants (WWTP), and the amount of sludge is growing due to the rapid urbanization and industrialization. For example, a production of 3.71 Mt of sludge in dry matter from WWTP was estimated for 2010 in China [1]. Landfill has played a major role in the disposal of sludge worldwide. Nevertheless, the public awareness of environmental issues, cost effective and renewable disposal possibilities are of concern.

Different treatments are used for sludge processing. Among of these processes, landfill, thermochemical, agricultural utilizing, aerobic digestion and composting have developed to a certain extent. However, the thermochemical process is considered promising ways in order to recover the potential energy and valuable products from sludge. As one of most important thermochemical technologies, pyrolysis was extensively used for the sustainable heat and power generation. However, the route of industrial process requires a better understanding of the physical and chemical characteristics of this thermal degradation. As pyrolysis is the thermal degradation of organic matters in oxygen free atmosphere to produce energy carrier materials like gases, bio-oil and char. it has advantages over conventional incineration with respect to fuel recycle, energy recovery and the control of heavy metal emissions. Many researchers have studied the effects of reaction conditions such as temperature, retention time, and heating rate on the yield and composition of the derived products from dried sewage sludge [2–4]. And various pyrolysis methods were carried out on biomass or sewage sludge such as the thermogravimetric analysis [5,6], slow pyrolysis [7,8], fast pyrolysis [9–11] or microwave-assisted pyrolysis [7,12–14]. According to the difference of moisture ratio, dried sewage sludge [15] and wet sewage sludge [16,17] were often used as samples to evaluate the kinetics with different thermal analysis methods for obtaining reasonable pyrolysis mechanisms. Zhang et al. [18] have developed a preliminary mechanistic to investigate the products variance of wet sewage sludge decomposition and the formation of intermediates during the pyrolysis process. Domínguez et al. [19] compared microwave and conventional pyrolysis of dried and wet sewage sludge in the production of syngas and pay attention to the generation of greenhouse gases. The influence of the raw material and moisture content on the gas composition was also evaluated. Although the solid materials of original wet sludge and dry sludge are similar, the pyrolysis of wet sludge directly will lead to three problems. First, high moisture content caused high energy consumption in the pyrolysis reactor. Second, water condensation will cause much more liquid products, which will lead to extra cost for purifying the products. Third, the partial pressure of H_2O in the reactor of wet sludge pyrolysis is far higher than the one in dry sludge pyrolysis reaction, and this might cause the switching of

* Corresponding author. Tel.: +86 411 84707448; fax: +86 411 84706679.
E-mail addresses: nbgao@dlut.edu.cn (N. Gao), leeam@dlut.edu.cn (A. Li).

0165-2370/$ – see front matter © 2013 Elsevier B.V. All rights reserved.
http://dx.doi.org/10.1016/j.jaap.2013.10.002

products composition. So, dry sludge pyrolysis might be suited for sludge mining. Additionally, several studies have been carried out on various reactors, such as fixed bed, fluidized bed, moveable bed, rotary kiln, and the heating rate of flash, fast or low pyrolysis was also practiced [20].

Regardless of the numerous studies on sewage sludge pyrolysis were carried, few studies focused on the process products analysis during the pyrolysis of dried sewage sludge, and furthermore, the intermediate products and the structure of functional groups of sludge pyrolysis has often been neglected. As the thermal degradation of the sludge is a complex process and a number of consecutive and parallel reactions are involved, the mechanistic insights on the behaviors of dried sludge pyrolysis and detailed investigation on the pyrolysis products at different working conditions are not very clear. The aim of this study is using TG–DSC, TG–FTIR, XRF and a tubular pyrolyzer for the dried sludge pyrolysis to explore the variation of functional group and products distribution.

2. Experimental

2.1. Materials

The dried sewage sludge used in this study was collected from drying plant in Dalian, China. The proximate and ultimate analysis of sludge samples were shown in Table 1. The proximate analysis of sewage sludge samples was measured by an automatic proximate analyzer (SDTGA5000, Sundy, China). The moisture, ashes and volatile matter were measured according to the ASTM standard test method no. E871, D1102 and E872. Ultimate analysis was performed with a CHNS/O elementary analyzer (Elementar, VarioEL III, Germany), oxygen (O) obtained by difference to 100%.

The mineralogical data of the samples of dried sewage sludge and pyrolyzed chars were analyzed by X-ray fluorescence (XRF) Spectrometer (Shimadzu XRF-1800, Japan). The major and environmentally most important elemental analysis of dried sewage sludge was displayed in Table 2. 26 elements were identified in the sludge. Compared with results in the literature [21], the sludge samples studied consisted of more P and S, which might attribute to nutrient substance.

2.2. TG–FTIR

Thermogravimetric–Fourier transform infrared analysis (TG–FTIR) experiments were performed by TG 209 thermogravimetric analyzer system (Netzsch, Germany) coupled with a Vertex70 spectrometer Fourier transform infrared spectrometer (FTIR) (Bruker, Germany). In this study, during the detection, approximately 10–20 mg of dried sewage sludge was heated in TG equipment with N_2 atmosphere at 10 °C min^{-1} of heating rate from 30 °C to 800 °C. The carrier gas (N_2) flow rate was 30 mL min^{-1}. The differential thermogravimetric (DTG) curves were obtained by numerical derivation of the TG curves. The gaseous products from the pyrolysis of sewage sludge in TGA were determined using FTIR spectra which were controlled by a Bruker spectrometer model Vector 22. The transfer line and gas cell were heated at a temperature of 200 °C to avoid the condensation of volatile decomposition products. The wave number range of IR was 4000–600 cm^{-1}. The resolution and sensitivity were set at 4 cm^{-1}, and the spectrum scan frequency was 8 times per minute.

2.3. Pyrolysis experimental procedures

A horizontal tubular furnace reactor was used in this study (see in Fig. 1). A quartz boat was placed inside the tubular reactor to load samples. N_2 was used as purging gas during the pyrolysis process. The N_2 flow rate is 2 L/min. The dried sewage sludge was ground

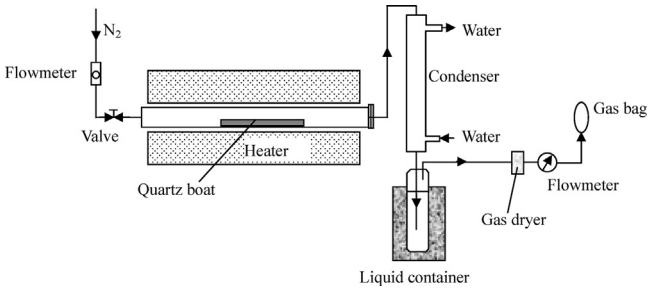

Fig. 1. Diagram of tubular pyrolysis reactor.

by grinding mill and sieved through around 20 mesh. 120–200 g dried sewage sludge were placed in the reactor. Pyrolysis temperatures ranged from 450 to 650 °C with 50 °C of increments. The sewage sludge pyrolysis experiments under fast and slow heating rates were investigated. The heating rate of slow pyrolysis was 8 °C min^{-1}, and the fast pyrolysis is 100 °C min^{-1}. Pyrolysis gases were collected by gas bags after a cooling unit. Wet gas meter was used to record the flow of the pyrolysis vapor during the pyrolysis experiments. The pyrolytic tar was collected by an Erlenmeyer flask at the tail of the cooling unit. The char was weighted after the complete cooling of the reactor.

The pyrolysis gas was periodically collected by the gas bag and analyzed off-line by gas chromatograph (GC). The pyrolysis gas mainly about H_2, N_2, CO, CH_4, CO_2, C_2H_4, C_2H_6, C_3H_8, and C_3H_6, was identified by the gas chromatograph with a thermal conductivity detector (TCD), a flame ionization detector (FID) and an injector connected to two 5 m length, 3 mm diameter columns helium was used as carrier gas.

2.4. Calculation of kinetic parameters

The pyrolysis kinetics of organic materials were described by first order Arrhenius law [22]. The integral method (Coats and Redferm [23]) was used to calculate the activation energy of the non-isothermal degradation of sewage sludge.

The basic kinetics analysis can be expressed as:

$$\frac{d\alpha}{dt} = k(T)f(\alpha) \tag{1}$$

where α is the conversion of the sewage sludge at the time t (s), which can be defined as,

$$\alpha = \frac{m_0 - m_t}{m_0 - m_f} \tag{2}$$

where m_t is the weight at any time t, and m_0 is the initial weight at the start of that stage, and m_f is the final weight at the end of that stage. $f(\alpha)$ is differential form of the kinetic model. k is rate constant, which is given by the Arrhenius equation: $k = A\exp(-E/RT)$, A is a pre-exponential factor (min^{-1}), E is apparent activation energy (kJ mol^{-1}), T is reaction temperature (k), R is gas constant (8.314 J mol^{-1} °C^{-1}) [24].

$f(\alpha)$ is presented as,

$$f(\alpha) = 1 - \alpha \tag{3}$$

Under a heating rate $\beta = dT/dt$, Eq. (1) is changed as,

$$\frac{d\alpha}{dT} = \frac{A}{\beta}(1-\alpha)\exp(-E/RT) \tag{4}$$

According to the approximate expression of Coats–Redfern method, Eq. (4) can be re-arranged and integrated as follows,

$$\ln\left[\frac{-\ln(1-\alpha)}{T^2}\right] = \ln\left[\frac{AR}{\beta E}\left(1-\frac{2RT}{E}\right)\right] - \frac{E}{RT} \tag{5}$$

Table 1
Proximate and ultimate analysis of samples.

Sample	Volatiles (%)	Fixed carbon (%)	Moisture (%)	Ash (%)	C (%)	H (%)	N (%)	S (%)	O[a] (%)
Sludge	59.06	9.36	7.5	24.08	36.45	5.93	7.03	0.77	25.74

[a] By difference.

Table 2
Mineralogical analysis of sewage sludge and pyrolysis residue (dry basis).

wt%	P	Si	Ca	Fe	K	S	Al	Cu	Mg	Zn	Na	Sn	Ti	Cl
Sludge	3.77	2.63	2.35	1.89	1.56	1.26	1.14	0.97	0.92	0.37	0.21	0.16	0.13	0.11
Residues	4.30	3.64	1.79	1.62	1.50	1.30	1.22	0.64	0.35	0.30	0.24	0.15	0.11	0.71

mg/kg	Cr	Mn	Ba	Ni	La	Ce	I	Sr	Zr	Co	Br	W
Sludge	930	612	560	409	378	329	223	167	133	81	48	47
Residues	661	514	469	311	231	208	84	47	–	–	–	–

As $\exp(-(E/RT)) \approx 0$, Eq. (5) can be simplified as,

$$\ln\left[\frac{-\ln(1-\alpha)}{T^2}\right] = \ln\left(\frac{AR}{\beta E}\right) - \frac{E}{RT} \quad (6)$$

Eq. (6) gives a plot of $\ln[-\ln(1-\alpha)/T^2]$ versus $1/T$ for various heating conditions should yield a straight line, whose slope is $-E/R$ and Y intercept is $\ln(AR/\beta E)$. The value of α, and T at any times could be obtained from the experimental TG and DTG curves. Thus, the apparent activation energy E and the pre-exponential factor A, could be determined from the above method [25].

3. Results and discussion

3.1. Thermal analysis

Fig. 2 shows the thermogravimetric (TG), differential thermogravimetric (DTG) and differential scanning calorimetry (DSC) curves for dried sewage sludge as a function of the temperature at a heating rate of 10 °C min^{-1} at nitrogen atmosphere. In the TG–DSC curves, three distinct regions were identified. The initial weight loss of 5.05% is related to the loss of physically absorbed water molecules in the temperatures lower than 120 °C. The maximum rate of water loss occurred at 87.6 °C from DSC curve. Correspondingly, an endothermic peak appeared, 133.6 J g^{-1} of heat was absorbed by water evaporation. The second weight loss region occurred in the range of 130–492 °C, about 66.72% of the total weight of sewage sludge weight loss. It is well known that this temperature range is the volatilization of volatiles in sewage sludge, and this is a rough judgment boundary for the main component decomposition in sewage sludge. In this stage, two strong loss rates occurred at 276 and 333 °C, and a deceleration period was followed until 492 °C. It presented two different types of organic volatiles were generated in the sewage sludge. The reason might be due to the ingredient such as proteins and carboxyl groups in the sewage sludge decomposition at approximately 300 °C [26]. From the DSC curve, in the stage of 276–454 °C, a significant exothermic peak was observed, and a total heat of about 169 J g^{-1} was produced. This might due to the not only proteins and the carboxyl groups decomposition but the cracking of carbon refractories such as aromatic ring, N-alkyl long chain structures and some saturated aliphatic chains [16]. In the temperature range from 492 to 720 °C, sewage sludge sample showed a weight loss of 9.00% of its original mass, slowly approaching a final residue weight of 44.23%. This stage might be attributed to the decomposition of inorganic materials, such as calcium carbonate [27,28]. Previous reported that sludge contained a large amount of inorganic materials such as calcium [27]. This period was marked by an approximately constant for the rate of weight loss. While the DSC curve in this temperature stage shows a continued endothermal process. This might be due to the polycondensation of C—C boned and C—O boned occurred in this temperature range. Finally, the solid residue of sewage sludge (carbonaceous residues within inorganic solid particles) was 44.23% of its original mass. A narrow endothermal peak was observed from the DSC curve in the temperature range from 469 to 512 °C, this might be due to some intermediate products took place secondary decomposition. And this process released endothermic heat of 11.22 J g^{-1}.

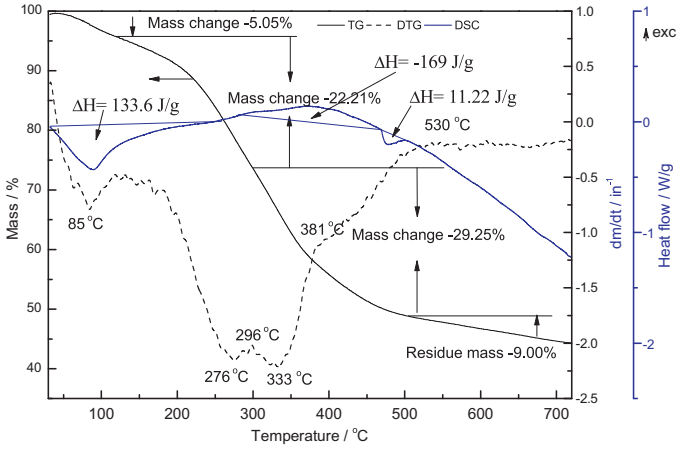

Fig. 2. TG, DTG and DSC curves for the dried sewage sludge during pyrolysis.

3.2. Kinetic analysis

The activation energy and pre-exponential factors of non-isothermal analysis of sewage sludge pyrolysis by TG–FTIR was presented in Table 3. High correlation coefficients indicated that the first order reaction model fits the experimental data very well. Combined with Fig. 2, two weight loss peaks were presented in pyrolysis reaction in two temperature ranges of 186–296 °C and 296–518 °C. The activation energy and frequency factor of the first weight loss peak (in the temperature of 186–296 °C) were 82.28 kJ mol^{-1} and 3.55×10^7 min^{-1}, respectively. While for the second weight loss, the values of activation energy and frequency factor were 48.34 kJ mol^{-1} and 8.04×10^2 min^{-1}, respectively. These results were in agreement with the report of Surjit Singh [23].

Table 3
The kinetic analysis of sewage sludge pyrolysis.

Reaction	Temperature range (°C)	E (kJ mol^{-1})	A (min^{-1})	Correlation coefficient, R^2
Pyrolysis	186–296	82.28	3.55×10^7	0.9797
	296–518	48.34	8.04×10^2	0.9394

3.3. Three dimension FTIR spectra analysis

Fig. 3 shows the three-dimensional FTIR spectra obtained from the gas volatized during the thermal decomposition of sewage sludge in a nitrogen atmosphere at a 10 °C min^{-1} of heating rate. In this figure, the vertical axis is absorbance units, the horizontal axis represents in wavenumbers and the perspective axis is the temperature. The pyrolysis gas was evolved between 200 and 700 °C. According to the TG curve in Fig. 2, an FTIR stack plot of spectra obtained at the representative temperature of 233 °C, 301 °C, 363 °C, 467 °C and 696 °C are shown in Fig. 4. The main gases identified by the characteristics wave numbers were methane (3025–3000 cm^{-1}), carbon dioxide (2400–2250 cm^{-1}), carbon monoxide (2200–2000 cm^{-1}) and some organic volatile compounds such as aldehydes and acids (1820–1660 cm^{-1}), alcohols and phenols (980–950 cm^{-1}).

As seen in Fig. 4, the evolved gases of sewage sludge were identified by their characteristic absorbance. The gas emission mainly occurred between 200 and 700 °C, which is in agreement with the thermogravimetric data. Distinct absorbance peaks were displayed in the region of 2400–2260 cm^{-1}, which is representative of CO_2 due to its indicative asymmetric stretching of the carbonyl group (C=O). In the temperature range of 150–367 °C, the absorbance increased quickly and reached a peak at 320 °C and then decreased gradually until 367 °C, which should be considered as the primary decomposition of organic volatile substance such as carboxyl occurring. This could be corresponding to the peak of the weight loss rate in the DTG curve occurring at 333 °C. The slight temperature difference was disagreement with the trend of TG curve. This might be due to the transferring retardation and the inverse mixing diffusion of evolved gases, which caused the delay and deforming of spectral signal [24]. After 529 °C, the CO_2 presented an increasing tendency up to 800 °C. In this stage, the polymerization reaction of coking in solid phase is primary reaction and some carbonate and oxygen-containing functional groups decomposed [29], and the continuous emission of CO_2 accompanies the whole stage. The absorbance bands of C—H stretching at 3100–2810 cm^{-1} indicate CH_4 evolved. The CH_4 absorption started around 221 °C then accelerated until reaching a maximum at 363 °C and decelerated until disappearing near 503 °C. The absorbance bands were shown in the wave numbers 1550–1286 and 3905–3645 cm^{-1}, which presents H_2O evolved. Water would be produced throughout the whole reaction process. The emission of water follows two steps. First, the absorbed water is released by evaporation below 150 °C. Secondly, as the temperature was beyond 200 °C, water was generated by the cleavage of aliphatic hydroxyl groups [30]. The emission of ammonia was confirmed by the appearance of absorption peaks at 964 and 930 cm^{-1} corresponding to N—H stretching vibration produced by the cleavage of nitrogen heterocyclic rings and the amount of hydrogen free radicals [29,30]. The absorbance bands of C—O stretching vibration at 2200–2000 cm^{-1} related to the release of CO increased with increasing temperature in the range of 232–482 °C caused by the decomposition of decarboxylation and other organic compounds cracking such as phenol, ether, ester, aldehyde and alcohol which contains oxygen functional groups [31]. The appearance of bands between 1680 and 1780 cm^{-1} confirmed the presences of carbonyl groups (formaldehydes, acetaldehyde and propionaldehyde) in the evolved gases during the pyrolysis of sludge. The inconspicuous absorbent peak

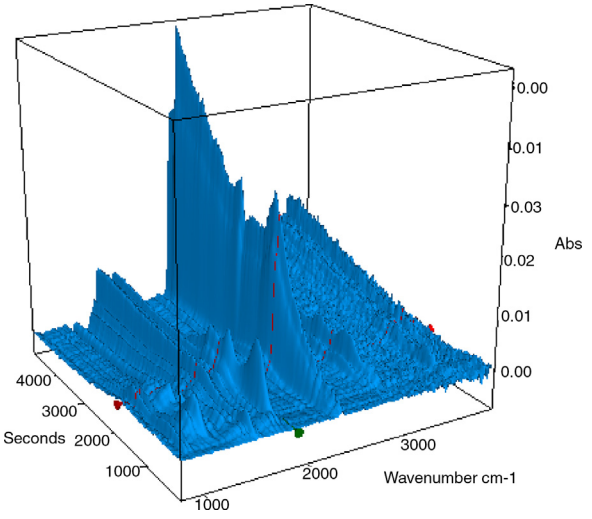

Fig. 3. Three-dimensional FTIR spectra of evolved gases from the pyrolysis of sewage sludge at a heating rate of 10 °C min^{-1}.

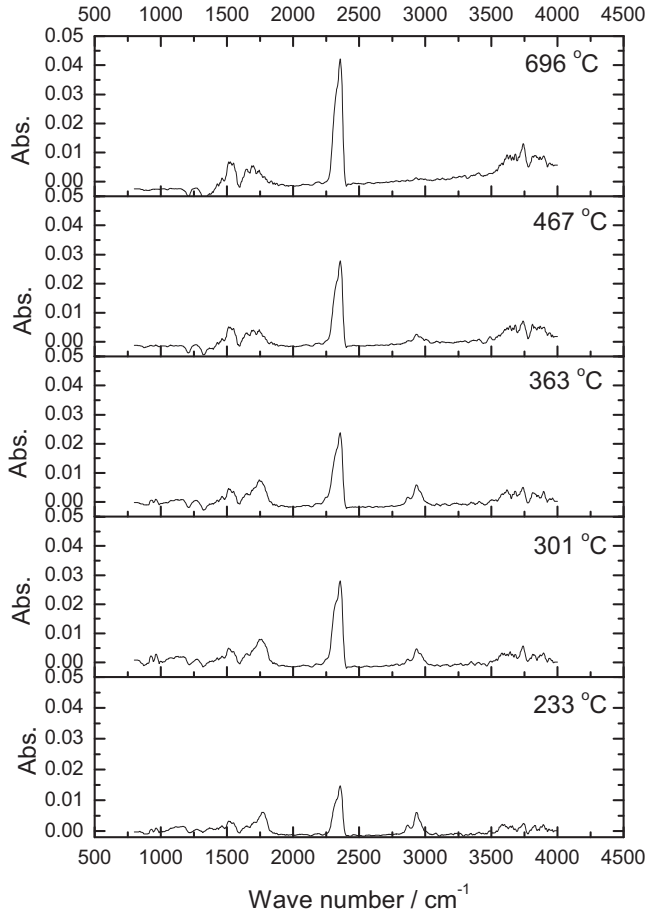

Fig. 4. FTIR stack plot of the evolved gases from pyrolysis of sewage sludge at a heating rate of 10 °C min^{-1}.

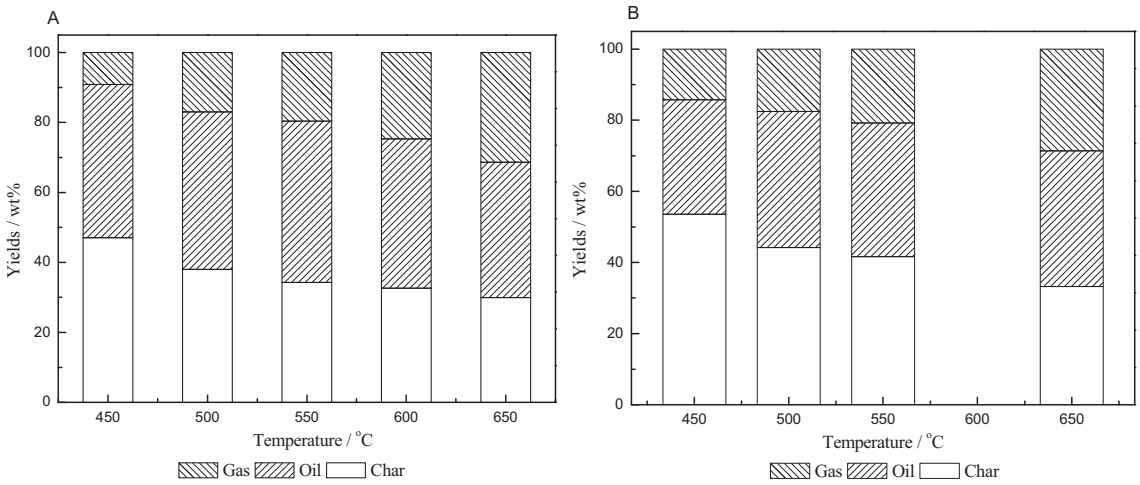

Fig. 5. Pyrolysis products yields under fast pyrolysis (A) and slow pyrolysis (B).

appeared in 985–950 cm^{-1} showed very little amount of alcohols and phenols evolved.

3.4. Products distribution of sewage sludge pyrolysis in tubular reactor

Fig. 5 showed the product distribution of sewage sludge pyrolysis under fast pyrolysis (A) and slow pyrolysis (B) in the temperature range of 450–650 °C at an interval of 50 °C. Under the heating rate of fast pyrolysis (Fig. 5(A)), char yields decreased from 47.07% at 450 °C to 29.96% at 650 °C with increasing pyrolysis temperature indicating that more tars and gases were released. While the yields of tar, which was condensable phase of the tar vapors, presented a slight rise between 450 and 550 °C and decreased when the pyrolysis temperature further increase. The maximum tar yield was 46.14% when the pyrolysis temperature was 550 °C. The temperature for maximum tar production was similar to the results of Lilly Shen et al. [3]. The trend might be due to the tar secondary reaction such as organic bonds' cracking, which become active at 550 °C or higher. The secondary reaction increased led to the gas yields production increased. So the gas yield was getting higher as increasing the pyrolysis temperature.

For the slow pyrolysis (Fig. 5(B)), the tar yields showed a little fluctuation trend in the range of 32.18–38.28%. This might be the result of the vapor was condensed into tar before the organic bonds were broken. The chars yield decreased from 53.60% in 450 °C to 33.24% in 650 °C, and the yield of gases showed an inverse trend, which increased from 14.24 to 28.64% with increasing temperatures from 450 to 650 °C. According to the appearance of tars, the fast pyrolysis tars were thicker than the slow pyrolysis ones. It might be caused by more macromolecule organics cracked under fast pyrolysis. In general, the tar yield under fast pyrolysis was more than that under slow pyrolysis, and the char yield was less than under slow pyrolysis conditions. This is in agreement with the other study [32].

The product gases (N_2 free) of sewage sludge pyrolysis included H_2, CO, CO_2, CH_4, and C_2—C_3 hydrocarbons (C_2H_4, C_2H_6, C_3H_6 and C_3H_8). The compositions of producer gas under fast and slow heating rates were shown in Table 4. For fast pyrolysis, the concentrations of all gases increased steadily with the increase of pyrolysis temperature from 450 to 650 °C except for CO_2. The concentrations of CO_2 decreased sharply as the pyrolysis temperatures increased from 450 to 650 °C. A possible reason for these results was the tars took place secondary reactions and the char was formed further. In these reactions, macromolecule organics cracked and micromolecule gases were produced. But the concentration of CO_2 decreased with the pyrolysis temperatures declined, this might result from the following reaction:

$$CO_2 + C = 2CO \quad (7)$$

In the case of higher pyrolysis temperature, CO_2 reacted with activated carbon and was transformed into CO. Another reason of CO_2 decline is that the macromolecular organic matters might be cracked into small ones such as H_2, CO, CH_4 and C_2—C_3 easily in higher temperatures.

The slow pyrolysis was similar to the fast pyrolysis. It also appeared this trend that the concentrations of H_2, CO, CH_4, and C_2—C_3 rised while CO_2 decreased. The results also presented that at 450–500 °C, the concentration of all gases varied very fast, but it was changed very slowly above 500 °C. When the pyrolysis temperatures were under 500 °C, the thermolable component like proteins and carboxyl groups cracked and the content of this organic matter

Table 4
Pyrolysis gas composition under fast and slow heating rate.

	Temperature (°C)	Gas composition (mol%)				
		H_2	CO	CO_2	CH_4	C_2—C_3
Fast pyrolysis	450	8.96	6.16	70.55	5.97	8.35
	500	18.95	16.49	41.9	11.98	10.68
	550	19.16	17.02	32.85	16.45	14.52
	600	17.73	17.12	23.81	20.5	20.85
	650	22.29	17.29	19.81	20.66	19.94
Slow pyrolysis	450	10.41	6.89	74.17	3.25	5.29
	500	12.46	14.13	41.9	19.58	11.93
	550	17.93	9.81	36.81	17.36	18.08
	650	26.9	9.8	31.95	19.87	11.48

was high, so the reaction rate was very fast. But the decomposition of the refractory produced above 500 °C, at the same time, the decomposition of the thermolable component might be induced because it was exothermic reaction resulting in a slower reaction rate.

The elemental compositions of the pyrolyzed sewage sludge residues obtained from XRF analyses are illustrated in Table 2. The dominant inorganic elements in sludge residue were P, Si, Ca, Fe, K, S and Al. Heavy metals showed different retrieval ratios in the sludge residues. The contents of cadmium and mercury were less than the limits of detection, which might be due to the highly volatile features. Considering the potential toxicity and high concentration levels, heavy metals of cancer-causing ingredients, such as nickel, lead, cobalt and cadmium should be paid special attention to be treated depending on their speciation [30,33].

4. Conclusions

The TG–FTIR results showed that the main decomposition temperature was in the range 186–518 °C. The activation energies of dried sewage sludge was 82.28 kJ mol^{-1} (186–296 °C) and 48.34 kJ mol^{-1} (296–518 °C), respectively. The main gaseous components identified by FTIR were methane, carbon dioxide, carbon monoxide and some organic volatile compounds such as aldehydes, acids, alcohols and phenols. In the tubular pyrolysis experiments, the maximum tar yield obtained was 46.14% at the temperature of 550 °C under fast pyrolysis condition. The concentrations of pyrolysis gases increased steadily with increasing the pyrolysis temperature from 450 °C to 650 °C except for CO_2. XRF results indicated that the dominant inorganic elements in sludge pyrolyzed residue were P, Si, Ca, Fe, K, S and Al.

Acknowledgments

The work cited in this paper was supported by the National Natural Science Foundation of China (NSFC) (51006018), the Fundamental Research Funds for the Central Universities (No. DUT13LAB08) and by an open foundation of State Key Laboratory of Multiphase Complex Systems (No. MPCS-2011-D-11).

References

[1] W. Wang, Research on Indirect Film Drying and Thermal Press Dewatering and Drying of Municipal Dewatered Sludge, Dalian University of Technology, 2012.
[2] L. Shen, D.-K. Zhang, Fuel 82 (2003) 465.
[3] L. Shen, D.-k. Zhang, Fuel 84 (2005) 809.
[4] M. Inguanzo, A. Domı´nguez, J.A. Menéndez, C.G. Blanco, J.J. Pis, Journal of Analytical and Applied Pyrolysis 63 (2002) 209.
[5] A.G. Barneto, J.A. Carmona, J.E.M. Alfonso, J.D. Blanco, Journal of Analytical and Applied Pyrolysis 86 (2009) 108.
[6] M. Muñoz, M.F. Gomez-rico, R. Font, Journal of Analytical and Applied Pyrolysis (2013), http://dx.doi.org/10.1016/j.jaap.2013.01.001.
[7] O. Mašek, V. Budarin, M. Gronnow, K. Crombie, P. Brownsort, E. Fitzpatrick, P. Hurst, Journal of Analytical and Applied Pyrolysis 100 (2013) 41.
[8] S. Uçar, S. Karagöz, Journal of Analytical and Applied Pyrolysis 84 (2009) 151.
[9] G. Yildiz, M. Pronk, M. Djokic, K.M. van Geem, F. Ronsse, R. van Duren, W. Prins, Journal of Analytical and Applied Pyrolysis (2013), http://dx.doi.org/10.1016/j.jaap.2013.02.001.
[10] D.J. Nowakowski, A.V. Bridgwater, D.C. Elliott, D. Meier, P. de Wild, Journal of Analytical and Applied Pyrolysis 88 (2010) 53.
[11] H.S. Choi, D. Meier, Journal of Analytical and Applied Pyrolysis 100 (2013) 207.
[12] Q. Lin, G. Chen, Y. Liu, Journal of Analytical and Applied Pyrolysis 94 (2012) 114.
[13] Q.H. Lin, H. Cheng, G.Y. Chen, Journal of Analytical and Applied Pyrolysis 93 (2012) 113.
[14] A.A. Salema, F.N. Ani, Journal of Analytical and Applied Pyrolysis 96 (2012) 162.
[15] X. Yang, Z. Jiang, Bioresource Technology 100 (2009) 3663.
[16] J. de Oliveira Silva, G.R. Filho, C. da Silva Meireles, S.D. Ribeiro, J.G. Vieira, C.V. da Silva, D.A. Cerqueira, Thermochimica Acta 528 (2012) 72.
[17] S. Xiong, J. Zhuo, B. Zhang, Q. Yao, Journal of Analytical and Applied Pyrolysis (2013), http://dx.doi.org/10.1016/j.jaap.2013.05.003.
[18] B. Zhang, S. Xiong, B. Xiao, D. Yu, X. Jia, International Journal of Hydrogen Energy 36 (2011) 355.
[19] A. Domínguez, Y. Fernández, B. Fidalgo, J.J. Pis, J.A. Menéndez, Chemosphere 70 (2008) 397.
[20] P. Manara, A. Zabaniotou, Renewable and Sustainable Energy Reviews 16 (2012) 2566.
[21] I. Velghe, R. Carleer, J. Yperman, S. Schreurs, Journal of Analytical and Applied Pyrolysis 92 (2011) 366.
[22] Y.F. Huang, W.H. Kuan, P.T. Chiueh, S.L. Lo, Bioresource Technology 102 (2011) 3527.
[23] S. Singh, C. Wu, P.T. Williams, Journal of Analytical and Applied Pyrolysis 94 (2012) 99.
[24] Y. Zheng, D. Chen, X. Zhu, Journal of Analytical and Applied Pyrolysis. (2013), http://dx.doi.org/10.1016/j.jaap.2013.05.018
[25] N. Gao, A. Li, C. Quan, L. Du, Y. Duan, Journal of Analytical and Applied Pyrolysis 100 (2013) 26.
[26] O. Francioso, M.T. Rodriguez-Estrada, D. Montecchio, C. Salomoni, A. Caputo, D. Palenzona, Journal of Hazardous Materials 175 (2010) 740.
[27] S.A. Scott, J.S. Dennis, J.F. Davidson, A.N. Hayhurst, Fuel 85 (2006) 1248.
[28] C. Casajus, J. Abrego, F. Marias, J. Vaxelaire, J.L. Sánchez, A. Gonzalo, Chemical Engineering Journal 145 (2009) 412.
[29] L. Tao, G.-B. Zhao, J. Qian, Y.-k. Qin, Journal of Hazardous Materials 175 (2010) 754.
[30] T. Ahamad, S.M. Alshehri, Journal of Hazardous Materials 199–200 (2012) 200.
[31] M.A. Lopez-Velazquez, V. Santes, J. Balmaseda, E. Torres-Garcia, Journal of Analytical and Applied Pyrolysis 99 (2013) 170.
[32] I. Fonts, G. Gea, M. Azuara, J. Ábrego, J. Arauzo, Renewable and Sustainable Energy Reviews 16 (2012) 2781.
[33] A.B. Hernandez, J.-H. Ferrasse, P. Chaurand, H. Saveyn, D. Borschneck, N. Roche, Journal of Hazardous Materials 191 (2011) 219.